Hybrid optoacoustic and ultrasound biomicroscopy monitors laser-induced tissue modifications and magnetite nanoparticle impregnation

Héctor Estrada[1], Emil Sobol[2],Olga Baum[2] and Daniel Razansky[1,3*]

[1]Institute for Biological and Medical Imaging (IBMI), Helmholtz Zentrum München, Ingolstädter Landstraße 1, 85764 Neuherberg, Germany
[2]Institute on Laser and Information Technologies, Russian Academy of Sciences, Moscow (Troitsk), Russia
[3]Faculty of Medicine, Technische Universität München, Ismaninger Straße 22, 81675 Munich, Germany

E-mail: *dr@tum.de

Abstract. Tissue modification under laser radiation is emerging as one of the advanced applications of lasers in medicine, with treatments ranging from reshaping and regeneration of cartilage to normalization of the intraocular pressure. Laser-induced structural alterations can be studied using conventional microscopic techniques applied to thin specimen. Yet, development of non-invasive imaging methods for deep tissue monitoring of structural alterations under laser radiation is of great importance, especially for attaining efficient feedback during the procedures. We developed a fast scanning biomicroscopy system that can simultaneously deliver both optoacoustic and pulse-echo ultrasound contrast from intact tissues and show that both modalities allow manifesting the laser-induced changes in cartilage and sclera. Furthermore, images of the sclera samples reveal a crater developing around the center of the laser-irradiated spot as well as certain degree of thickening within the treated zone, presumably due to pore formation. Finally, we were able to observe selective impregnation of magnetite nanoparticles into the cartilage, thus demonstrating a possible contrast enhancement approach for studying specific treatment effects. Overall, the new imaging approach holds promise for development of noninvasive feedback control systems that could guarantee efficacy and safety of laser-based medical procedures.

PACS numbers: 87.85.Pq, 81.70.Cv, 42.62.Be

1. Introduction

Tissue modification under laser radiation is emerging as one of the advanced applications of lasers in medicine, with treatments ranging from laser correction of septonasal deformities [1], laser reconstruction of spine disks and joints [2, 3] to non-destructive normalization of the intraocular pressure in glaucomatous eyes [4]. Indeed, in many cases, the low level laser therapies allow replacing traumatic surgeries with low-invasive procedures. Yet, safety and efficacy of laser modification technologies rely on efficient feedback control systems to accurately monitor the changes in tissue structure. To this end, laser-induced structural alterations have been mainly studied ex-vivo using conventional microscopic techniques applied to thin specimen, including histological methods [3], atomic force microscopy and electron microscopy [4, 5]. Various non-destructive techniques, including light scattering measurements [5, 6], optical coherence tomography (OCT) [7], and ultrasound imaging [8, 9], have been also applied to study laser-treated tissues. While the optical methods may generally attain high-resolution contrast from superficial tissue layers, intense light scattering in deeper structures hinders their implementation in depth-resolved imaging of bulk living tissues. Ultrasonography was shown to manifest good structural contrast from deep layers of cartilage and sclera tissues [8]. In the context of laser treatments, ultrasound-based imaging might further become a promising candidate for monitoring of laser-induced formation of submicron size pores in cartilage matrix, which has been recently established as one of the factors promoting regeneration of cartilaginous tissues [3]. Similarly, formation of gaseous pores in laser-treated sclera allows substantially increasing its water permeability, serving as a basis for new types of glaucoma therapies [4]. By means of a optoacoustic imaging approach, which uses intense short-duration laser pulses to induce ultrasonic responses in deep tissues layers [10], a real-time feedback capability during laser treatments was recently showcased, yet only reported for monitoring of destructive laser ablation procedures [11]. In this work we present a newly developed fast scanning biomicroscopy system that can simultaneously deliver both optoacoustic and pulse-echo ultrasound contrast from intact tissue volumes. The system is subsequently evaluated in visualizing structural alterations in laser-treated cartilage and sclera. Furthermore, we investigate the use of biofunctional magnetite nanoparticles (NP) for enhancing contrast in cartilage diagnostics. Here the driving hypothesis has been the significantly slower penetration of NPs sized above 10 nm into healthy cartilage versus damaged areas of the tissue [12], which may allow monitoring of spatial distribution and dynamics of NP impregnation.

2. Materials and Methods

2.1. The hybrid imaging system

The hybrid fast-scanning system is based upon a coaxial design, which enables simultaneous acquisition of both laser-induced and pulse-echo ultrasound responses from the imaged object (Fig. 1). The scanning head consists of an ultrawideband spherically-focused Polyvinylidene Fluoride (PVdF) ultrasound transducer having active diameter of 6 mm and 7.8 mm focal length (Precision Acoustics, Dorchester, United Kingdom). To ensure propagation of ultrasonic waves, the scanning head and the imaged object are submerged into a small container filled with water serving as an acoustic coupling medium. A photonic crystal single mode fiber (LMA20; NKT

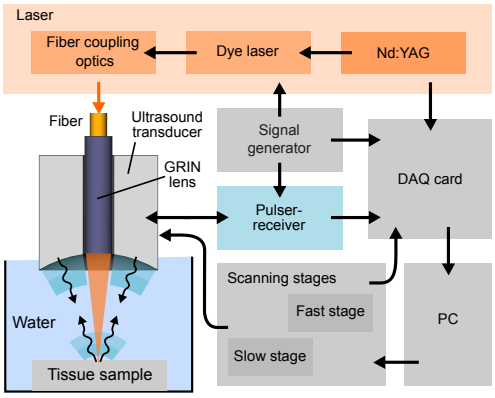

Figure 1. Diagram of the hybrid optoacoustic-ultrasound imaging system. The diagram in the left bottom corner depicts the hybrid coaxial scanning head.

Photonics A/S, Birkerød, Denmark), pigtailed with a Gradient-Index (GRIN) lens (Grintech GmbH, Jena, Germany) is inserted coaxially through a 0.8 mm diameter opening in the center of the transducer aperture. The fiber-lens assembly can form a diffraction limited focal spot at a distance of 7.1 mm from the transducer surface. In this way, an optical-resolution optoacoustic microscopy image can be formed by delivering focused laser pulse and detecting the ultrasound waves emanating from the sample due to the light absorption. Short pulsed laser light (pulse duration of 8 ns) with up to 20 μJ per-pulse energies is delivered to the imaged object from a Dye Laser (Model: Credo; Sirah Lasertechnik GmbH, Grevenbroich, Germany) fed by a diode end pumped Nd:YAG Q-switched laser (Model: IS8II-E; EdgeWave GmbH, Wrselen, Germany). In this way, by selecting the appropriate dye cassette, the laser pulses can be generated in a broad wavelength range between 540 nm to 800 nm and a maximum repetition frequency of up to 10 kHz. Correction of the laser pulse energy fluctuations is further performed using continuous photodiode measurements. The ultrasound data is subsequently acquired by the same transducer operated in a pulse-echo mode by emitting and receiving the ultrasound waves reflected by the sample. For this, the transducer is fed by 6 ns duration pulses generated by an ultrasonic pulser/receiver (5073PR, Olympus), which is also responsible for amplification of the measured optoacoustic and ultrasonic responses before digital sampling is performed by the data acquisition (DAQ) card (Model: M3i.4142; Spectrum Systementwicklung Microelectronic GmbH, Grosshansdorf, Germany). Real-time scanning and three-dimensional data acquisition is achieved by a fast linear piezoelectric stage (model M683; Physik Instrumente GmbH, Karlsruhe, Germany) mounted on top of slower linear stage (model LTM 60F; Owis GmbH, Staufen, Germany). This implementation allows for scanning rates of between 10 to 30 B-scans per second, depending on the field of view within the specimen. A typical three-dimensional scan is achieved within several seconds. Storage of the measured data and control of the scanning stages is performed using a personal computer (PC).

2.2. Image formation and post-processing methods

The three-dimensional image volume for both optoacoustic (OA) and ultrasound (US) data is rendered by nearest neighbour interpolation of the zigzag trajectory of the scanning head into a regular two-dimensional grid and the projection of the recorded time-resolved acoustic signals onto the depth dimension. While the exact locations in the lateral plane are accurately calibrated by the scanning stages, the depth dimension is calculated using the proportionality between the ultrasound time of flight and the propagation distance assuming constant speed of sound in water. Thus, the depth of the OA reconstructed volumetric image is calculated as $z = ct$ and for the pulse-echo ultrasound image as $z = 2ct$. In addition, the measured signals have been high-pass filtered with cut-off frequency at 1 MHz to avoid unwanted low-frequency offsets. The detected OA signals were corrected for pulse-to-pulse energy variations of the laser using the signal from a calibrated photodiode located in the vicinity of the fiber output. To enable maximizing contrast in the images, histogram equalization has been applied to the reconstructed volume, which has the largest signal-to-noise ratio (SNR). Then, the same adjusted colour map is used for all other volumes with lower SNR, which permits a direct relative comparison between the signals in different images. Besides these post-processing steps, no other filtering or reconstruction algorithms have been applied to the raw OA and US data.

2.3. Preparation of samples

Costal cartilage and eye sclera tissues were used for the ex-vivo experiments. Twenty samples of fresh porcine costal cartilage were prepared using a scalpel as layers measuring 3±0.1 cm in length, 7.0±0.5 mm in width, and 3.0±0.5 mm in thickness. Five of the samples were not irradiated by the laser and remained intact throughout the experiments. Other samples were continuously irradiated for 6 s with a 2.5 mm diameter beam from a continuous wave laser at a wavelength of 1.56 μm, instantaneous power of $P = 2.2$ W, pulse duration of 500 ms, and pulse repetition rate of 1.4 Hz. These particular settings have been previously established as the optimum for stable reshaping of costal cartilage for transplantation avoiding thermal damage and denaturation [13]. Nevertheless, in order to investigate overheated cartilage, four cartilage samples were also irradiated with 40% higher power levels of $P = 3$ W. All specimens were kept in physiological solution for 15 minutes before experiments and stored in 10% neutral formalin thereafter. For contrast-enhanced imaging, both intact and irradiated samples of porcine costal cartilage were subsequently impregnated by magnetite nanoparticles (NPs) for 14 hours. NPs were prepared according to the procedure described in [12]. Experiments on sclera were performed ex-vivo on four eyes of two mini-pigs using pulse repetitive infrared laser radiation at 1.56 μm. Ten laser spots of 0.6 mm in diameter, instantaneous power of 0.9 W, pulse duration of 200 ms, and pulse repetition rate of 2 Hz were applied on the sclera at a distance of approximately 1-2 mm from the eye limb. As previously reported, this particular laser setting provided the thermo-mechanical effect necessary for efficient formation of pores, which resulted in a substantial increase of hydraulic permeability in the sclera [4]. This unique effect was further employed for a new type of safe and effective intraocular pressure (IOP) normalization technique relying on the enhancement of uveoscleral outflow under nondestructive laser irradiation of the sclera [4].

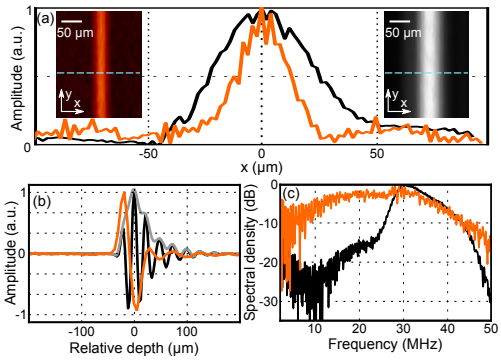

Figure 2. Characterisation of OA (orange) and US (black) modalities using a 10 μm polyamide suture. (a) MAP showing a lateral cross section of the suture. (b) Signal amplitude as a function of the depth relative to the transducer focus. The envelope of the US (black) signal appears in grey. (c) Frequency response of the OA and US signals from (b).

3. Results

3.1. Characterization of the hybrid imaging performance

A polyamide suture of 10 μm in diameter is used for the characterization of the hybrid OA and US microscope. As depicted in Fig. 2(a), the lateral resolution of OA system (right inset, orange curve) reaches 21 μm, in agreement with previously measured value of 20 μm [14], while the US counterpart reaches 48 μm (left inset, black curve). The axial resolution (Fig. 2(b)), measured as the width of the rising edge for the OA modality and as the full-width at half maximum of the US signal envelope (grey curve), yields 24 μm and 48 μm respectively. The intrinsic differences between the formation of the OA and the US images can be clearly distinguished in Fig. 2(c). While the spectrum of the detected OA signal abides the ultrawideband behaviour of the PVdF-based detector, the same object delivers a much narrower reflected spectrum when interrogated by means of a focused ultrasound wave. The relatively small diameter of the suture drastically reduces the amount of low frequency (long wavelength) components reflected back to the transducer, further justifying the lower than expected lateral resolution (48μm instead of 60 μm, as expected from the diffraction theory) as well as the ringing artefacts that decrease the axial resolution of the pulse-echo US imaging mode.

3.2. Imaging results in laser-treated cartilage

Differences between intact and laser-treated cartilage samples are evident in the OA maximum amplitude projection (MAP) images shown in Fig. 3 (a) and (c). Significant increase in the overall OA signal strength in the laser treated cartilage manifests laser-induced modification of cartilage structure not only inside the area encircled by the laser spot (white dashed circle), but also around the laser-irradiated zone where temperature gradients lead to thermo mechanical stress resulting in structural alterations, in particular formation of gas bubbles and pores [1]. The pore formation process further increases the thickness of the tissue sample in the laser-treated region,

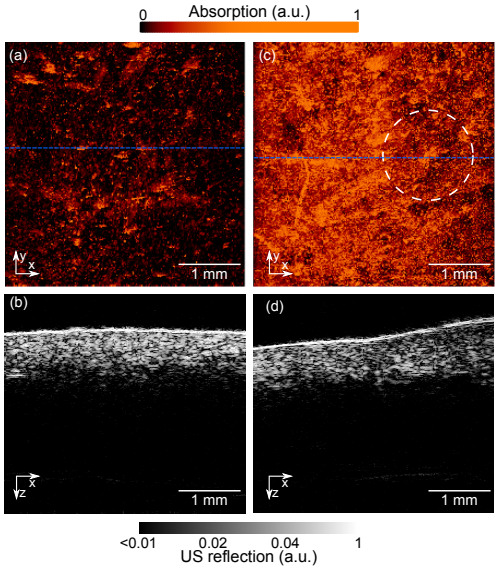

Figure 3. MAP OA images (top row) and US cross sections (bottom row) of non-irradiated (a), (b) and radiated cartilage (c), (d). The treated region lies within the white dashed circle in (c). The blue dashed lines in (a), (c) show the position of the US cross sections (b), (d) respectively.

as clearly manifested in the US B-scans (Fig. 3 (b), (d)), which were acquired along the cross-sectional plane depicted as a blue lines in Figs. 3(a) and 3(c). As expected, the latter reveal also the characteristic multilayered structure of cartilage. The bottom surface of the cartilage sample (≈3 mm thick) is barely visible due to the strong attenuation and scattering suffered by the ultrasound wave as it propagates from the detector and back.

3.3. Contrast enhancement with nanoparticle impregnation

OA images of the same laser treated sample before and after NP impregnation show clear differences due to the increase in the bulk optical absorption properties of the tissue, representing the main contrast for the OA modality (Fig. 4 (a), (d)). OA images show heterogeneity of NP impregnation due to the corresponding heterogeneity of the tissue structure. Generally, the OA contrast is expected to be dependent on the timing of NP impregnation and the particular laser settings used for the preliminary irradiation, which resulted in pore formation and creation of other defects in the cartilage structure. On the other hand, no significant differences can be seen in both MAP (Fig. 4(b) versus 4(e)) and B-Scan (Fig. 4(c) versus 4(f)) US images, testifying that the mechanical properties of the sample have not been modified. Yet, the size and localization of the structural defects due to laser irradiation are clearly manifested with the US images. Thus, combined OA and US imaging facilitates accurate monitoring of spatial distribution of NP impregnating into cartilage through laser-induced pores or other defects of cartilage structure.

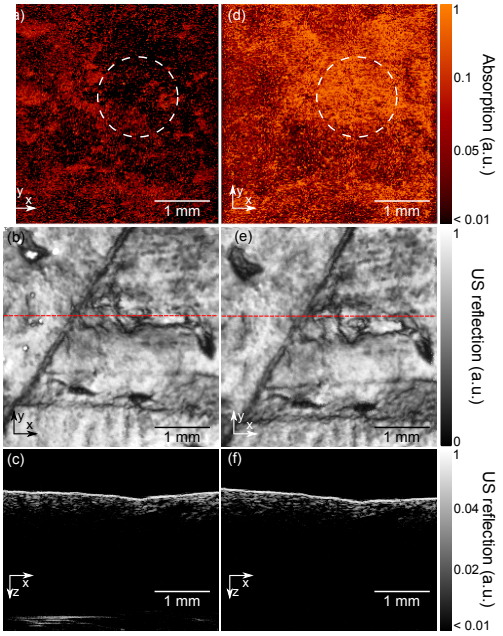

Figure 4. OA MAP (top row), US MAP (middle row), and US cross sections (bottom row) images of a laser-treated cartilage before (left column) and after (right column) NP impregnation by soaking in NP suspension for 14 hours. The position of the treated region is marked with a white dashed circle. Red dashed lines in the US MAP show the position of the US cross sections.

3.4. Imaging of the laser-treated sclera

Intact sclera is characterized with nearly isotropic structure, which can be clearly verified in the corresponding images shown in Fig. 5. Both US and OA images exhibit laser-induced structural alterations in the sclera, including heterogeneity of the structural modifications, more pronounced near the laser-irradiated spot, as well as formation of gaseous pores and crater-like structure on the irradiated surface. While OA microscopy allows for high-resolution monitoring of the laser-induced pore system, US imaging additionally delivers information on dynamics of the sample thickness due to formation of pores and craters, which can be used to establish optimal laser power and exposure time profiles not resulting in undesirable modification of the sclera.

4. Discussion and conclusions

The newly developed fusion between fast scanning optoacoustic and pulse-echo ultrasound biomicroscopy modalities was used here for visualization of changes induced by low-level laser radiation in cartilage and sclera. The observed effects correlate well with the common conclusions rendered via histological, AFM and light scattering examinations of cartilage that underwent non-destructive laser treatment for reshaping or regeneration [3, 13, 15] as well as sclera where laser irradiation is used for enhancing water permeability in intraocular pressure normalization procedures [4, 16]. Yet, the suggested methodology may potentially bring another dimension into those

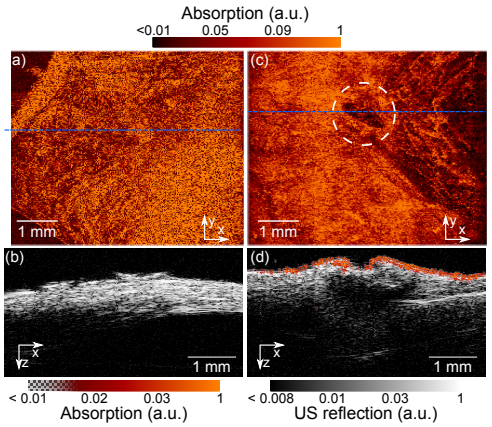

Figure 5. OA MAP (top row) and OA-US cross sections (bottom row) images of intact (left) and enhanced power laser treated sclera (right). The position of the treated region is depicted by a white dashed circle. Blue dashed lines show the position of the cross sections.

observations by enabling high resolution three-dimensional imaging deep inside intact tissues at different spatial scales and with both mechanical and optical contrast. Furthermore, we were able to attain usable contrast by monitoring spatial distribution of NP impregnating into cartilage through laser-induced pores as well as the dynamics of NP impregnation, which can be exploited for early diagnostics of cartilage diseases [12]. By imaging tissues impregnated with NP of specific size distribution, one can target for early diagnostics of arthritis and other cartilage-related diseases which otherwise cannot be manifested today using MRI and other conventional imaging methods. It was recently established that laser-induced formation of pores in the sclera may serve as a basis for new approaches toward IOP normalization in glaucoma [4], however, no monitoring approach currently exists that can deliver an efficient feedback necessary for determining settings for optimal pore formation in IOP normalization procedures. The hybrid OA and US microscopy was able to visualize laser-induced formation of pores in the eye sclera, which can be potentially used to dynamically adjust the laser irradiation settings in order to prevent undesirable modification of the sclera structure. In the current system implementation, the images suffer from reduced penetration ability, especially in the OA mode. Yet, these are not hard limitations and it is well anticipated that further improvements to the optical illumination strategies noise reduction algorithms will be able to significantly extend the effective imaging depth. In addition, both the US and OA modalities might benefit from improved image reconstruction algorithms that properly account for out-of-focus signals. In conclusion, the developed hybrid fast scanning system holds promise toward early diagnostics of cartilage diseases and creating monitoring and feedback control systems for increasing efficiency and safety of novel laser medical technologies for normalization of the intraocular pressure in ophthalmology and for cartilage repair in the ENT and orthopedics.

Acknowledgments

We gratefully acknowledge the valuable help of Moritz Kneipp in the sclera experiments. The research leading to these results has received funding from the European Research Council under grant agreement ERC-2010-StG-260991. The work was also supported by the Russian Foundation for Basic Research, grants 13-02-00435 and 12-02-00786.

References

[1] E N Sobol, T E Milner, A B Shekhter, O I Baum, A E Guller, N Y Ignatieva, A I Omelchenko, and O L Zakharkina. Laser reshaping and regeneration of cartilage. *Laser Physics Letters*, 4(7):488, 2007.

[2] Emil Sobol, Anatoly Shekhter, Anna Guller, Olga Baum, and Andrey Baskov. Laser-induced regeneration of cartilage. *Journal of Biomedical Optics*, 16(8):080902–080902–11, 2011.

[3] E.N. Sobol, A.B. Shekhter, and A.V. Baskov. Lasers in orthopaedic surgery. In Helena Jelínková, editor, *Lasers for Medical Applications*, Woodhead Publishing Series in Electronic and Optical Materials, pages 628 – 658. Woodhead Publishing, Cambbridge, UK, 2013.

[4] Olga I. Baum, Emil N. Sobol, Andrey V. Bolshunov, Anatoly A. Fedorov, Olga V. Khomchik, Alexander I. Omelchenko, and Evgenii M. Shcherbakov. Microstructural changes in sclera under thermo-mechanical effect of 1.56μm laser radiation increasing transscleral humor outflow. *Lasers in Surgery and Medicine*, 46(1):46–53, 2014.

[5] V.V. Tuchin and Society of Photo-optical Instrumentation Engineers. *Tissue Optics: Light Scattering Methods and Instruments for Medical Diagnosis*. Press Monographs. Society of Photo Optical, 2007.

[6] G.J. Müller. *Medical optical tomography: functional imaging and monitoring*. SPIE institutes for advanced optical technologies. SPIE Optical Engineering Press, 1993.

[7] D Huang, EA Swanson, CP Lin, JS Schuman, WG Stinson, W Chang, MR Hee, T Flotte, K Gregory, CA Puliafito, and al. et. Optical coherence tomography. *Science*, 254(5035):1178–1181, 1991.

[8] F.Stuart Foster, Charles J Pavlin, Kasia A Harasiewicz, Donald A Christopher, and Daniel H Turnbull. Advances in ultrasound biomicroscopy. *Ultrasound in Medicine and Biology*, 26(1):1 – 27, 2000.

[9] S Kaushik, S Kumar, R Jain, R Bansal, S S Pandav, and A Gupta. Ultrasound biomicroscopic quantification of the change in anterior chamber angle following laser peripheral iridotomy in early chronic primary angle closure glaucoma. *Eye*, 21(6):735–741, March 2006.

[10] Changhui Li and Lihong V Wang. Photoacoustic tomography and sensing in biomedicine. *Physics in Medicine and Biology*, 54(19):R59, 2009.

[11] Erwin Bay, Xosé Luís Deán-Ben, Genny A. Pang, Alexandre Douplik, and Daniel Razansky. Real-time monitoring of incision profile during laser surgery using shock wave detection. *Journal of Biophotonics*, 2013.

[12] YuliaM. Soshnikova, SvetlanaG. Roman, NataliaA. Chebotareva, OlgaI. Baum, MariyaV. Obrezkova, RichardB. Gillis, StephenE. Harding, EmilN. Sobol, and ValeriyV. Lunin. Starch-modified magnetite nanoparticles for impregnation into cartilage. *Journal of Nanoparticle Research*, 15(11):1–10, 2013.

[13] Olga I. Baum, Yulia M. Soshnikova, Emil N. Sobol, Andrey Ya. Korneychuk, Mariya V. Obrezkova, Valeriy M. Svistushkin, Oxana K. Timofeeva, and Valeriy V. Lunin. Laser reshaping of costal cartilage for transplantation. *Lasers in Surgery and Medicine*, 43(6):511–515, 2011.

[14] Héctor Estrada, Jake Turner, Moritz Kneipp, and Daniel Razansky. Real-time optoacoustic brain microscopy with hybrid optical and acoustic resolution. *Laser Physics Letters*, 11(4):045601, 2014.

[15] A V Yuzhakov, A P Sviridov, E M Shcherbakov, O I Baum, and E N Sobol. Optical properties of costal cartilage and their variation in the process of non-destructive action of laser radiation with the wavelength 1.56μm. *Quantum Electronics*, 44(1):65, 2014.

[16] Aleksey V. Yuzhakov, Alexander P. Sviridov, Olga I. Baum, Evgenii M. Shcherbakov, and Emil N. Sobol. Optical characteristics of the cornea and sclera and their alterations under the effect of nondestructive 1.56-m laser radiation. *Journal of Biomedical Optics*, 18(5):058003–058003, 2013.